FACULTY OF SCIENCES

A comparison of postcranial osteology and associated burrowing performance of four amphisbaenian morphotypes.

Ditte De Waele
Student number: 01501481

Supervisor: Prof. dr. Dominique Adriaens
Counsellor: Aurélien Lowie

Master's dissertation submitted in order to obtain the academic degree of
Master of Science in Biology

Academic year 2020-2021

GHENT UNIVERSITY

Introduction

Tetrapods, the ‘four legged’ animals, find their origin in the sea some 400 million years ago. With time, it allowed them to explore a vast new territory: land. Why then, have so many species evolved to lose their limbs? Limb loss in squamates is generally thought to be beneficial for burrowing or surface-dwelling locomotion (C. Gans, 1974). Limb loss occurred particularly often in Squamata. Squamata - the ‘scaled reptiles’ - is the largest reptile order, and comprises snakes (Serpentes), lizards and worm lizards (Amphisbaenia). Most amphisbaenians are limbless, and all are true burrowers, spending most of their time inside permanent burrows.

Amphisbaenians have remarkable cranial adaptations. Four main types of cranial shapes are reported: round-, shovel-, spade- and keel-shape (Figure 1). *Bipes*, a limbed amphisbaenian clade, has a round snout, as does the limbless *Blanus*; rhineurids and some others (e.g. *Monopeltis capensis*) are shovel-snouted; spade-shaped heads are found in trogonophids (e.g. *Trogonophis wiegmanni*); and eight amphisbaenid genera are keel-snouted (e.g. *Geocalamus acutus*). Each shape functions in an accordingly specialized method of head-first digging (C. Gans, 1974). Amphisbaenians with round heads simply burrow themselves in through forward pushes. Shovel-headed amphisbaenians, considered to be the most specialized species for digging (Hohl *et al.,* 2017), dig by pushing the head forward and upward, compressing the soil to the roof of the burrow, while their pectoral region compresses the tunnel floor. *Trogonophis wiegmanni*, spade-snouted, applies a unique burrowing method: it uses both vertical and rotational head movements, scraping soil off the walls and simultaneously compressing it against the walls with his head and body. Finally, the keel-snouted amphisbaenians push their pointed snout into the soil and press the soil sideways by moving the head left and right.

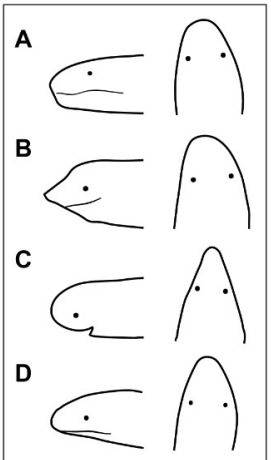

Figure 1: Illustration of four head morphotypes, lateral (left) and dorsal view (right). A - round; B, shovel; C, keel; D, spade.

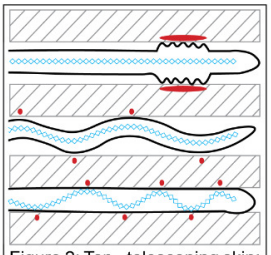
Figure 2: Top - telescoping skin; Middle - Whole-body concertina; Bottom - Internal concertina. Red dots: pressure points; Blue line: vertebral ccolumn

Amphisbaenian skin is composed of annuli encircling the trunk. They can expand their diameter, anchoring the skin against the tunnel walls. Skin and skeleton are only loosely connected, allowing forward and backward movement of the vertebral column. Hence, this is sometimes referred to as ‘telescoping’ (C. Gans, 1978; Figure 2).

Supposedly amphisbaenians use **internal concertina locomotion**. This mode was found in caecilians (limbless, elongated amphibians) (Herrel & Measey, 2010). So far, the sole amphisbaenian documented to use internal concertina is the shovel-headed *Leposternon microcephalum*, who uses it when moving backwards inside its burrows (Hohl *et al.*, 2014). External concertina locomotion is generally used on the surface. The body takes a wave-like shape, with the outer apices of each wave serving as a contact point (*point d’appui)*, from which it projects the body forward (or pulls the anterior part of the body forward). Internal concertina is similar to external concertina locomotion; the wave-shape is produced not by the entire body but solely by the vertebral column and attached musculature (Figure 2). Necessary for internal concertina locomotion, the vertebral column moves independent from the skin (vertebral bending while the skin remains elongated). This skin-vertebral independence is thought to disappear in narrow species (being very elongated), due to lack of coelomic space to generate bends (Summers & O’Reilly, 1997), however this hypothesis was tested and not confirmed for certain caecilians by Herrel & Measey (2010).

Generally, limbless animals have elongated bodies. Since larger animals require more energy to burrow into the ground, they remain restricted to having a relatively small diameter (Navas *et al*., 2004). Hence, their muscle mass is limited laterally. They can compensate for this limitation, increasing effective muscle cross-sectional area and muscle mass through elongation of the body and rearrangement of the muscle fibers. Elongation could be established through addition or elongation of vertebrae. In case of internal concertina locomotion, a higher number of vertebrae permits more acute bending and shorter wavelengths, increasing the degree of skin-vertebral independence (Herrel & Measey, 2010).

The postcranium could be adapted to burrowing in other ways besides number or length of vertebrae. Only little research has been done on the vertebral shapes in relation to limbless burrowing techniques. Mostly focus lay on the atlas-axis-occipital condyle skeletal bridge. Čerňanský & Stanley (2019) looked at atlas and axis shapes in dibamids and some amphisbaenians. In dibamids, which are limbless burrowing reptiles, the zygapophyseal articulation between atlas and axis is absent. Moreover, reduction of the transverse processes of the atlas was found to be associated with fossoriality. This is rather unexpected, as the muscles attached to these processes function to laterally rotate the head; with reduced transverse processes, the moment arm could be too short, making these movements ineffective (Čerňanský & Stanley ,2019).

Vertebrae posterior to the atlas-axis complex are usually similarly shaped, becoming more elongated posteriorly. Caudal vertebrae are an exception, having distinct processes (e.g. ventral processes called haemapophyses, or the anterolateral pleurapophyses). The posterior haemapophyses are fused, forming the haemal arch. Its lateral flanks used to be an attachment site for *m. caudofemoralis longus*, which functions as a hindlimb retractor (Otero *et al.*, 2012). Reduction of these lateral sides could therefore be expected in limbless reptiles.

Very little comparative research has been done on the vertebral shapes of amphisbaenians. The aims of this research are to determine the main axes of shape variation of selected vertebrae among four amphisbaenian species to investigate morphofunctional patterns in light of species' mode of burrowing and forces produced while burrowing.

Objective

Shovel-heads are considered the most specialized burrowers according to Hohl (2017) and C. Gans (1974). Round-headed amphisbaenians are considered 'generalized', and dig more shallow burrows compared to all other morphotypes. Hence, we expect our round-headed specimens to produce the smallest and our shovel-heads the largest burrowing forces.

Since elongation and limb reduction requires alterations to the musculature, possible changes in muscle insertion sites are of interest, specifically, for muscles associated in burrowing locomotion and muscles previously associated with limbs. However controversially, transverse processes of the atlas are found to be reduced in fossorial species (Čerňanský & Stanley, 2019). Since attached muscles function to rotate the head, species using rotational movement to excavate their burrows are expected to have less reduced transverse processes than species burrowing through forward pushing or mainly vertical head movements.

Depending on the burrowing method, an according degree of neck flexibility is imperative. Flexibility can be accomplished through many, not mutually exclusive, vertebral traits. Firstly, we expect zygapophyseal articulation between atlas and axis to be lost. This would permit a greater range of movements in the skeletal bridge between cranium and trunk, and is found in many serpentiform morphotypes (A. Čerňanský, 2016). Secondly, the condyle shape should allow for the rotations or

inclinations made by the head while burrowing. Hence, rounded condyles are expected in species using an oscillatory burrowing method (e.g. the spade-snouted *T. wiegmanni*) whereas compressed condyles serve as a hinge (ball-and-socket) for vertical or horizontal flexion of the head. Thirdly, when moving the head ventrad, the third intercentrum (i.e. the posterior of two hypapophyses on the axis) moves towards the ventral side of the third vertebra. Upon contact (minding there lies soft tissue in between), a long third intercentrum could block further ventrad movement. Therefore, morphotypes that rely on ventrad cranial movement (shovel- and spade-snouts) are expected to have a short third intercentrum.

We expect these vertebral traits to be less distinctive further along the vertebral column, since only the anterior part of the trunk is used for burrowing. Caudal vertebrae are expected to show little specializations to burrowing, except perhaps in our spade-snouted specimen, which relies on its tail for initial penetration of the soil.

Material & Methods

Subject animals

Four species were selected to have one of each head morphologies: *Blanus cinereus* (round), *Trogonophis wiegmanni* (spade), *Monopeltis capensis* (shovel, M. Kearney (2003)) and *Geocalamus acutus* (keel). Three of them were obtained from the personal collection of Anthony Herrel, Muséum National d'Histoire Naturelle, Paris. *Trogonophis wiegmanni* was obtained via Morphosource, an online 3D database (*www.MorphoSource.org*). All four are inhabitants of Africa. *T. wiegmanni* and *B. cinereus* live in northern parts of Africa; *M. capensis* occupies western regions, from Cameroon to Cape; *G. acutus* lives in Tanzania and Kenya (http://www.reptile-database.org/). All specimens are adults. A study by Hohl *et al.* (2017) pointed out that sex has no significant effect on the here studied traits, hence sex was not determined. All species prefer sandy soils as burrowing substrate, however, more specialized morphotypes (spade-, shovel-, keel-headed) can burrow in denser, less compressible soils than the generalized morphotype that is round-headed (C. Gans, 1974).

Body measurements

The specimens were weighed and the following morphometric data were collected for all four species using a digital caliper (Mitutoyo, ±0.1mm): snout-vent length (SVL), head length (HL), head width (HW), head height (HH), tail length (TL), body width (BW) and body height (BH). These data were collected to test for their correlation with vertebral shapes and burrowing forces generated by each morphotype (see Statistical analysis).

Burrowing trials & push force measurements

Of *Blanus cinereus*, 11 specimens were subjected to burrowing trials, for *Geocalamus acutus* 26. Due to limited finds in the field, of both *Monopeltis capensis* and *Trogonophis wiegmanni,* only 1 specimen performed the burrowing trials.

Forces generated by individuals while burrowing were measured with a force plate, according to the method described by Vanhooydonck *et al.* (2011) as follows: "Measurements of push forces during burrowing were made using a custom piezoelectric force platform (Kistler Squirrel force plate, +- 0.1 N). The force platform was positioned on a custom-designed metal base (Figure 3) and connected to a charge amplifier (Kistler Charge Amplifier type 9865). A Perplex block with 1 cm deep holes of different diameters was mounted on the force plate, level with the front edge (Figure 3). One of the holes was loosely filled with soil from the site where the specimens were found. A Perplex tunnel with a diameter similar to the maximal body diameter of the test animal was mounted on the metal base in front of (but not touching, see Figure 3) the force plate, and aligned with the soil-filled hole in the Perplex block. First, a specimen was introduced into the tunnel and allowed to move through it until reaching the soil-filled chamber." Next, the animal was stimulated to burrow by tapping the tail.

The exerted forces were recorded during a 60s recording session at 1000 Hz. Each animal was subjected to three trials, with at least 1h between trials. Forces were recorded in three dimensions. Of each trial, the maximum resulting force was calculated (where force in x, y and z-orientation were the cumulative largest, Figure A1). Since baseline forces (F0, when the animal is not pushing), tend to increase with time (noise on the detection), we chose the 'baseline force' as the force at the time of initiation of burrowing (T0). The overall maximum force for one specimen was calculated by averaging the three maximum forces (one for each trial).

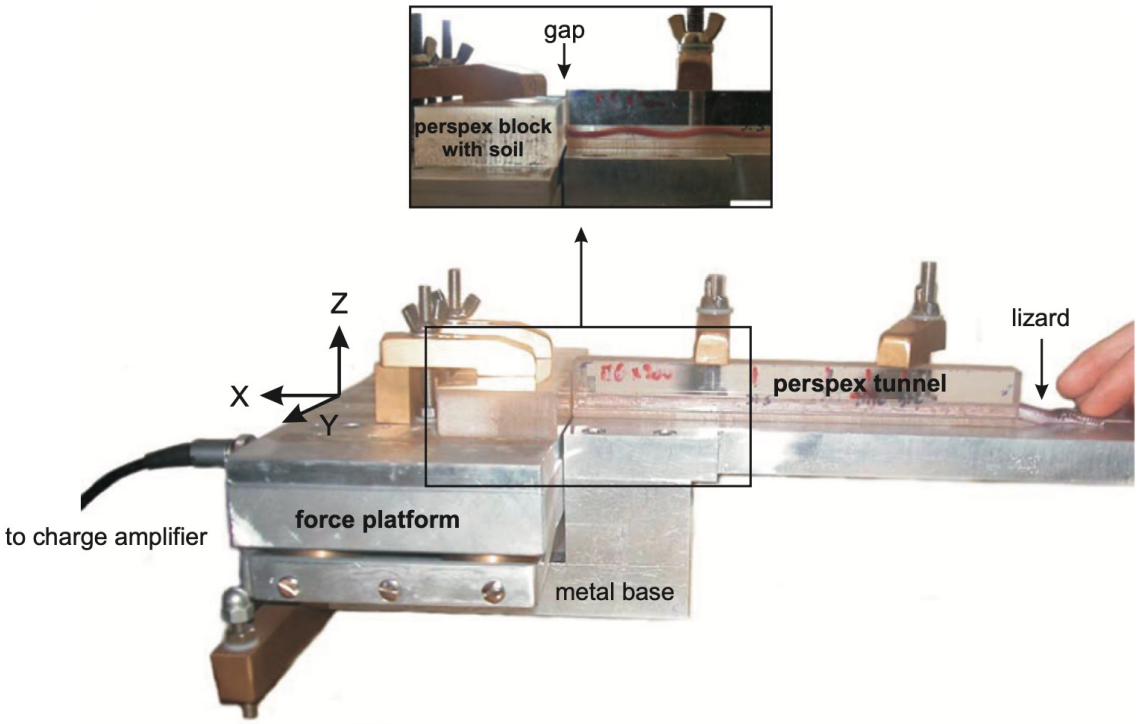

Figure 3: Set-up used to measure push forces, as published by Vanhooydonck *et al.* (2010). A specimen is placed inside the tunnel and stimulated to burrow his head into the soil-filled perplex block at the end of the tunnel. A force platform beneath the perplex block detects its push forces.

3D imaging and landmarking

Six vertebrae per specimen were selected for interspecies comparison. These six were: the atlas, axis and the first postaxis vertebra ("V1", "V2" and "V3" respectively), and a vertebra on 20, 60 and 90% of the total number of vertebrae ("V20", "V60" and "Caudal" respectively).

Each specimen was rolled in a jar and subjected to micro-computed tomography scanning. Of *Blanus cinereus, Geocalamus acutus* and *Monopeltis capensis*, µCT-scans were made at Ghent University with the Hector scanner (0.5-1mm aluminum filter; 100-200kV; 10-15W; averaging 2000 projections), equipped with a 240 kV X-ray tube from X-RAY WorX and a PerkinElmer 1620 flat-panel detector. *Trogonophis wiegmanni* was scanned at the University of Michigan Museum of Zoology, Research Museum Center using a Nikon XT H 225ST µCT Scanner (the files were downloaded from www.MorphoSource.org, where all data about the specimens, scanner settings and voxel sizes are available). Voxel sizes are listed in Appendix (Table A1).

The µCT-scans (.tiff files) were reconstructed as image stacks in ImageJ, downsized (from 16 to 8 bits), cropped and converted to .raw files as preparation for segmentation using Amira 5.5.

Segmented vertebrae were extracted (as .ply) and surfaces were smoothed using Geomagic Studio 12, after which the .ply files were ready for landmarking.

Landmarks will serve for statistical shape analysis and were placed using Stratovan Checkpoint x64 software. They were chosen to describe biologically meaningful features such as contacts between bones and tips of processes. The number of landmarks vary between vertebrae depending on where in the body the vertebrae are from (e.g. the atlas has 23 landmarks, the axis has 21; images of landmark placements are found in Figure 4).

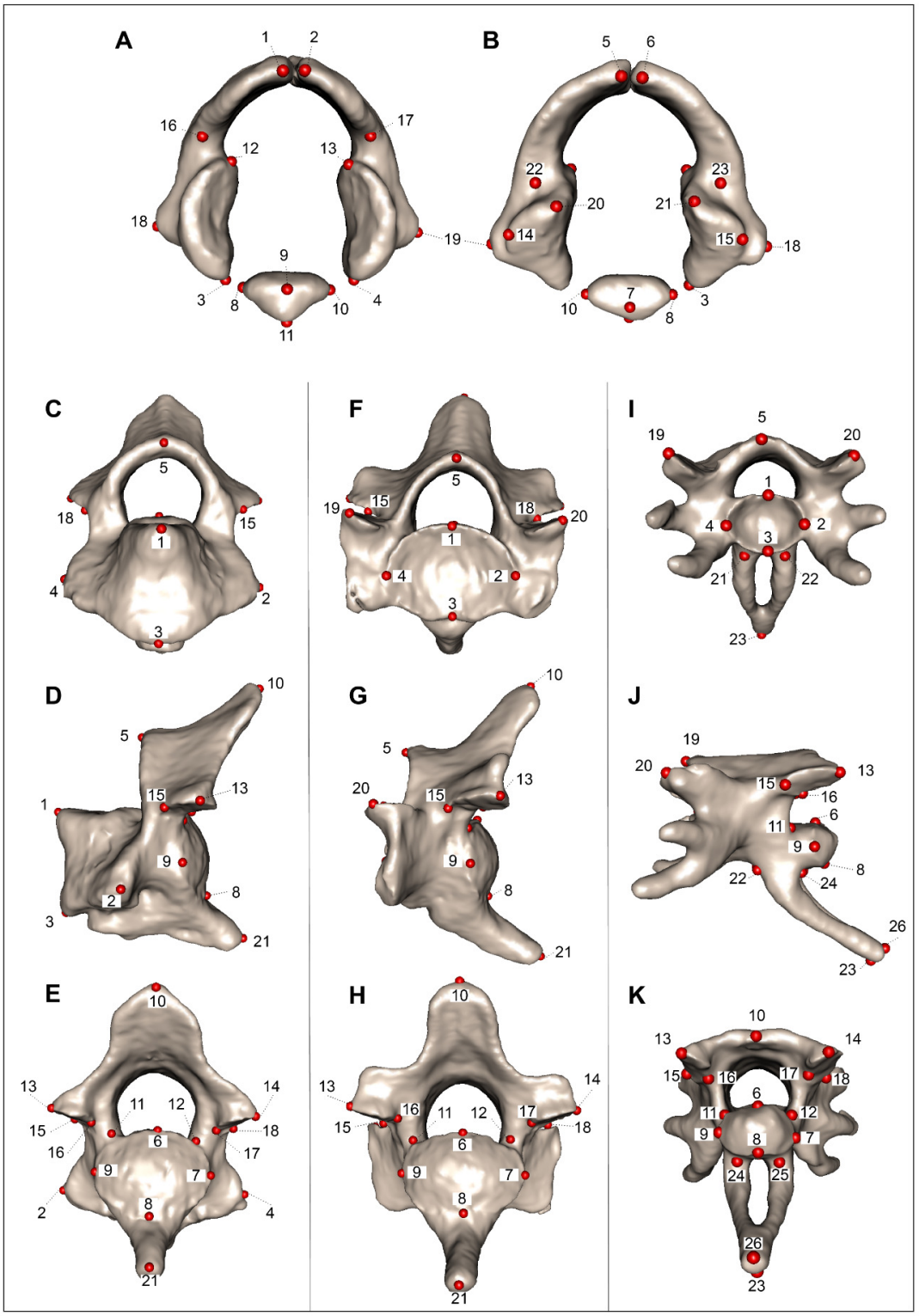

Figure 4: Placement of landmarks. A, B: Anterior resp. posterior view of the atlas (23 landmarks); C, D, E: Anterior, lateral and posterior view of the axis (21 landmarks); F, G, H: Anterior, lateral and posterior view of the third vertebra (V3, 21 landmarks). V3 landmarking is representative for landmark placement in V20 and V60 also,

except in V20 and V60 no landmark-21 was placed (as they lack a hypapophysis). V20 (20 landmarks), V60 (20 landmarks). I, J, K: Anterior, lateral and posterior view of the caudal vertebrae (26 landmarks).

Statistical analysis
All analysis and statistics were performed using R version 4.0.2.

Generalized Procrustes Analysis (GPA) with partial Procrustes superimposition was used on the 3D meshes to align the corresponding landmarks. Therefore, each shape was translated to the origin of the 3D plane, scaled to unit-centroid size and rotated to align homologous points (landmarks) as closely as possible.
Outliers were defined based on the Procrustes distances of each shape from the mean shape. Allometry was tested for using ordination least squares regression (OLS) on log10-transformed centroid sizes.
Principal component analysis (PCA) of the residuals (to adjust shapes for size) was used to visualize the main axes of morphological variation between the landmark configurations (function gm.prcomp in R). The number of principal components (PC's) to sufficiently describe the variation between shapes was determined to be two, based on the Scree test and the Bartlett-Lowley-Anderson test.

Morphometric data were log10-transformed to improve normality. Burrowing forces were linearly regressed against the body measurements to determine which measurements correlate with push force.

Multivariate linear regression analyses were used to assess relation between vertebral Procrustes shape coordinates, the measurement of interest resulting from previous linear regression, and push force (with interaction term). Both the shape coordinates and burrowing forces were then adjusted for the body measurement of interest. Ultimately, the relation between adjusted shapes and burrowing forces was tested for, through linear regression on their residuals.

Results

Figure 5 below shows several vertebrae with appointed terminology. Terminology of the vertebral structures follows mainly Čerňanský & Stanley (2019). In the Appendix (Figures A2-A7), a more extensive visualization of each vertebra for all four morphotypes is listed.

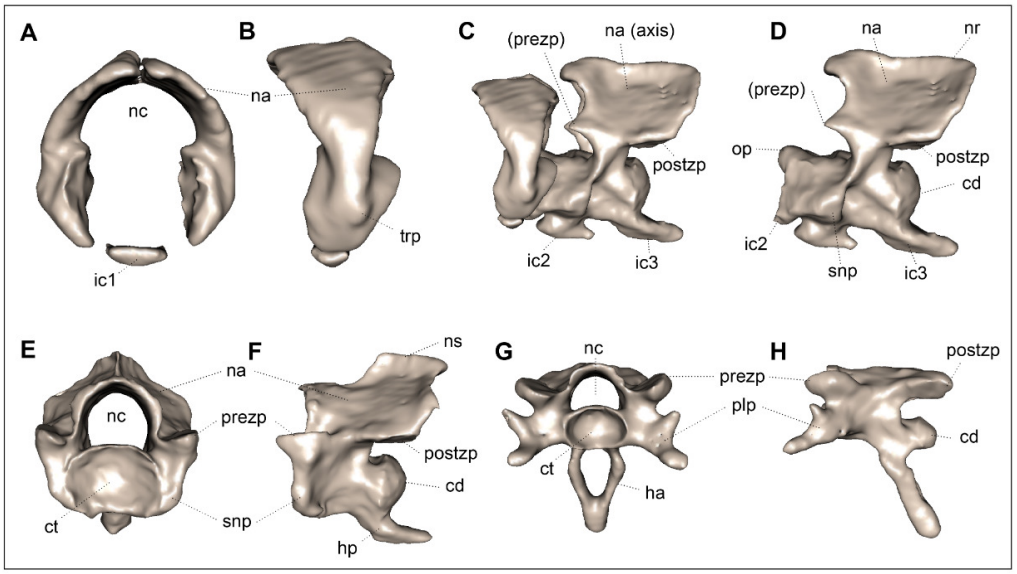

Figure 5: A, B: anterior and lateral view of the atlas; C: Lateral view of atlas + axis; D: Lateral view of the axis; E, F: Anterior and lateral view of V3; G, H: Anterior and lateral view of a caudal vertebra. Abbreviations: cd, condyle; ct, cotyle; ha, haemal arch; hp, hypapophysis; ic1, ic2 & ic3, intercentrum 1, 2 & 3; na, neural arch; nc, neural canal; nr, neural ridge; op, odontoid process; plp, pleurapophysis; postzp, postzygapophysis; prezp, prezygapophysis; trp, transverse process.

Outliers

No outliers were detected when each vertebral type was tested between four morphotypes. When V3 through caudal vertebrae were researched together, the V3 of *T. wiegmanni* was detected to be an outlier (Figure A8, left column).

Allometry

Procrustes ANOVA (999 permutations) to test shape variation and covariation in function of size resulted in a non-significant p-value for all vertebrae (Appendix Table A2). However, especially the graph depicting allometric relation in caudal vertebrae shows the four points approximating the diagonal, which suggests that shape does vary depending on size, i.e. there is allometry (Figure A2, right column). This illustrates how the test fails to detect a significant relationship due to the small sample size. Hence, despite the non-significant results for allometry, we proceded analysis of shapes adjusted for size.

Scree test

The scree test suggests to keep the first principal component only for all except V3 vertebrae and V3-V20-V60-Caudal vertebrae together (two PC's suggested). In theory, the second PC, as its eigenvalue lies below the corresponding broken stick component, can be omitted. However, Bartlett-Anderson-Lowley tests suggest using the first two or three PC's. We choose to use the first two PC's. Scree plots are listed in the Appendix (Figure A9).

Morphospace of the atlas (V1)

PCA for atlas shapes showed two principal components together explained 100% of the variation between species (Figure 6). The first principal component explains 76.77% of the total variance. Along this PC-axis, atlases become narrower and higher for higher PC1 scores. The minimal shape occurs for *M. capensis,* whose atlas is visibly wider than it is high. On the other end of the PC1-axis, we find *G. acutus*, whose atlas is higher than it is wide (Figure A2). PC1 also shows variance in the intercentrum shape. A hint of a keel progresses with higher scores.

The second PC depicts variation in the neural spine dorsal area and the intercentrum, accounting for the remaining 23.23% of the atlantal shape variation. For higher PC2 scores, the posterior side of the atlas neural spine moves ventrally and the front of the neural spine progresses, resulting in a broader neural spine. The intercentrum goes from horizontally flattened at low PC2 values to vertically flattened at high PC2 values. Intercentra are reduced in all four species, as is usual for amphisbaenians (Čerňanský & Stanley, 2019; Figure A2).

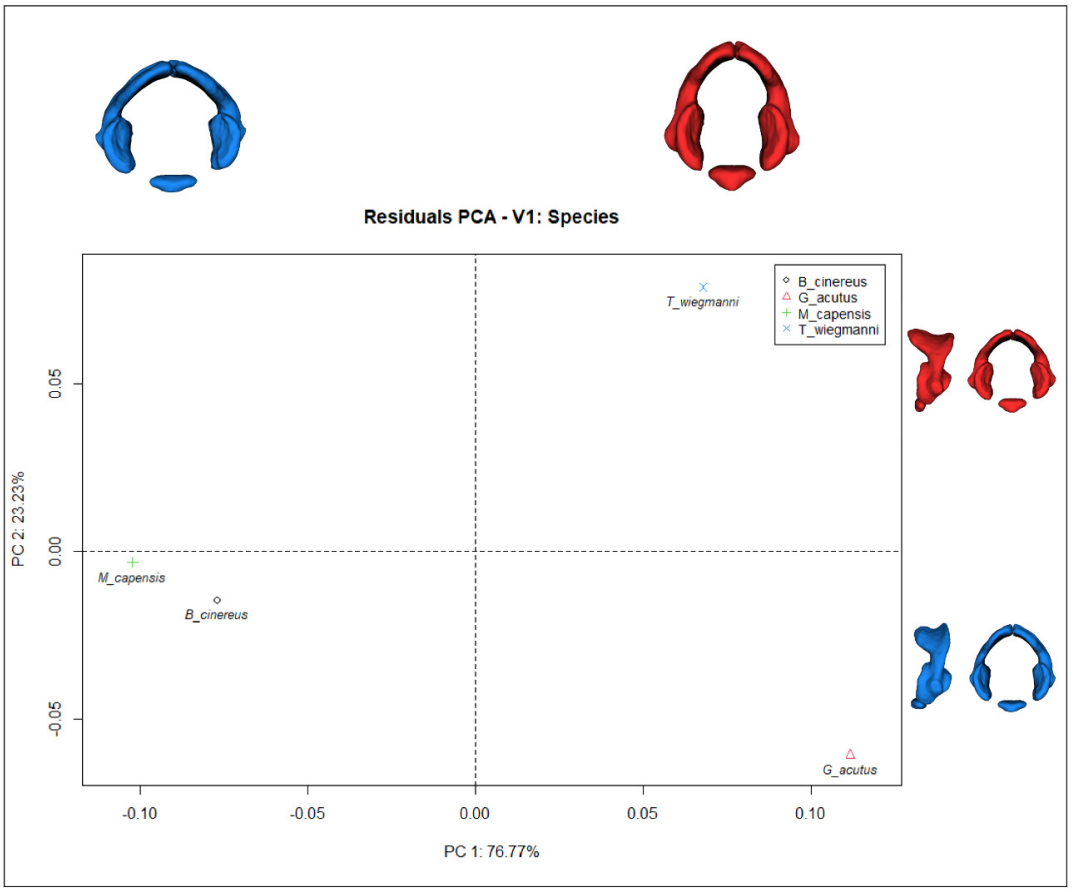

Figure 6: Major axes of atlantal shape variation. Blue: warped surfaces representing minimum shapes for the first two PC's. Red: warped surfaces representing maximum shapes.

Morphospace of the axis (V2)

For the axis vertebrae, basically all of the variation is explainable by the first to PC's (100%) (Figure 7). With higher PC1 scores, the vertebra becomes shorter and the posterior tip of the third intercentrum is positioned more ventrad. Positive scores for the second principal component show shortening of the third intercentrum and a lowered anterior tip of the neural arch, leaving a shorter, inclined rather than horizontal, neural ridge. *G. acutus* is the sole species with a negative score for PC2, having a horizontal neural spine and a relatively long 3rd intercentrum. The neural arch becomes laterally stretched with higher PC2 scores.

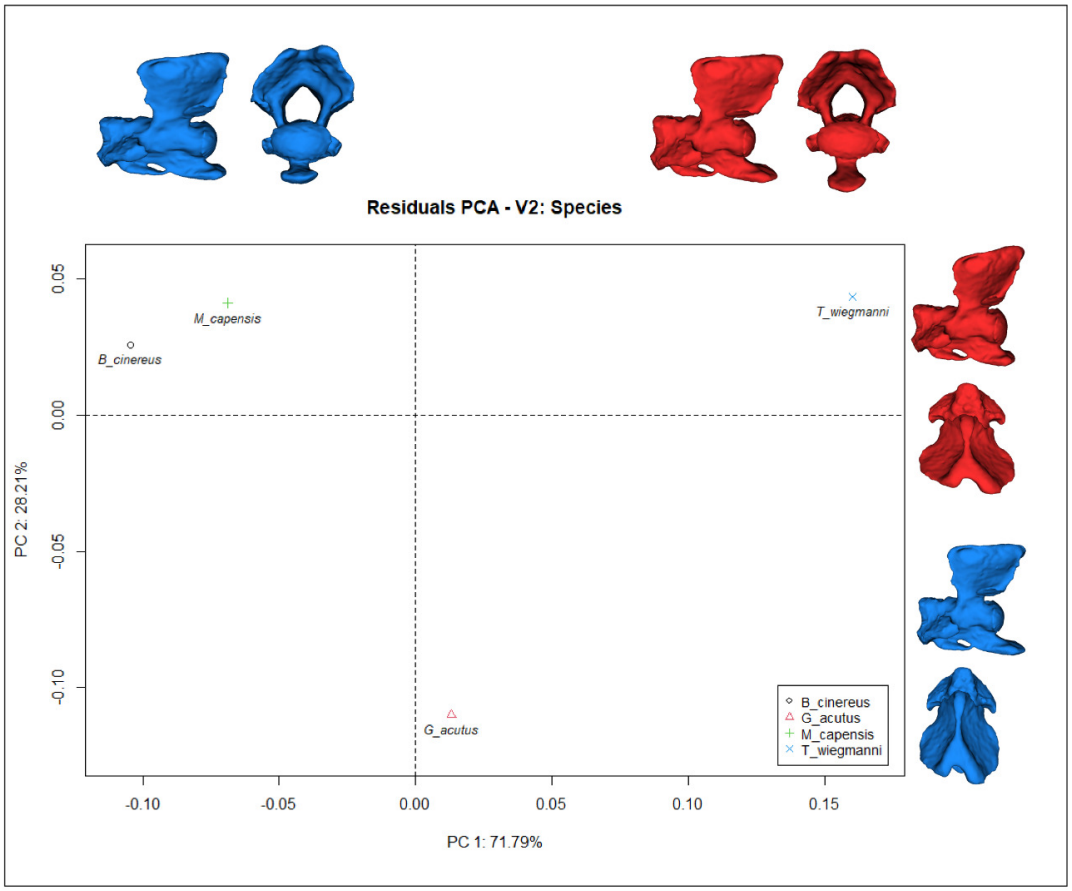

Figure 7: Major axes of axis shape variation. Blue: warped surfaces representing minimum shapes for the first two PC's. Red: warped surfaces representing maximum shapes.

Morphospace of the third cervical vertebra (V3)

The V3 morphospace (Figure 8) shows similar patterns of shape variation as found for the axis. I.e. PC1 shows increasing craniocaudal compression with increasing PC1 scores. This results in more laterally pointing prezygapophyses and a wider neural spine for vertebrae with high PC1 scores. The posterior apex of the hypapophysis moves ventrally. Together these traits explain 78.9% of total variation between the third vertebrae of the four morphotypes. Our spade-snout (*T. wiegmanni*) has the most ventrad oriented hypapophysis.

The second PC (21.15%) depicts variation in the position of the anterior apex of the neural spine and the length of the intercentrum. High PC2 scores accord with the apex pointing more anterior (compared to upward pointing for smaller scores) and with a shorter intercentrum. Only *G. acutus* has negative PC2 score, being the sole species whose V3 anterior neural spine tip is oriented dorsally.

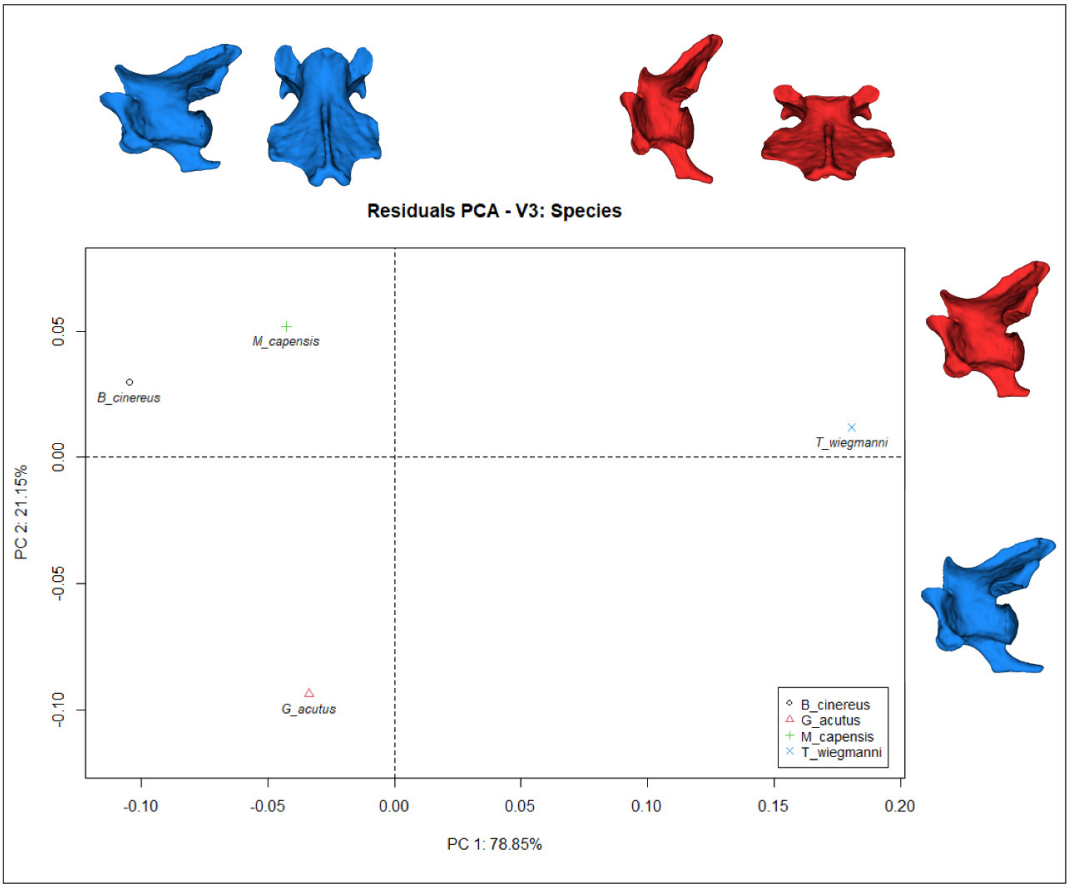

Figure 8: Major axes of V3 shape variation. Blue: warped surfaces representing minimum shapes for the first two PC's. Red: warped surfaces representing maximum shapes.

Morphospace of V20

90.12% of the total variance is mainly found in the length and width of the V20 vertebrae (Figure 9). Along the first PC-axis, vertebrae change from a square shape, viewed dorsally, being approximately equally long as wide, to a more elongated shape: with higher PC1-scores, length/width ratio increases and the prezygapophyses point forward rather than laterally. Further, variation is mainly found in the neural spine (the median ridge of the neural arch). PC2 accounts for 9.88% of total shape variation. Higher scores relate with an elevated neural spine tip.

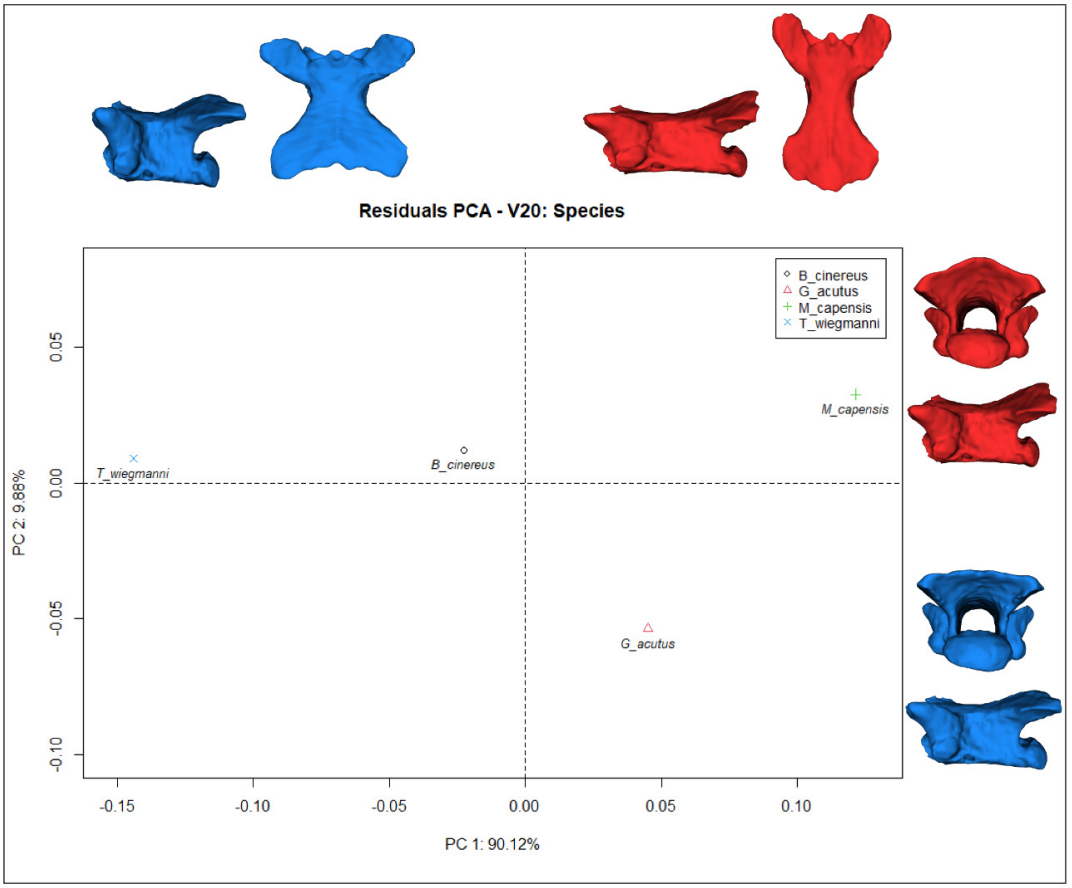

Figure 9: Major axes of V20 shape variation. Blue: warped surfaces representing minimum shapes for the first two PC's. Red: warped surfaces representing maximum shapes.

Morphospace of V60

Similar as for 20% vertebrae, PC1 of V60 vertebrae shows main shape variation occurs in the vertebral length and width of the vertebrae, with an increasing length/width ratio for higher PC1-values and, again prezygapophyses pointing more forward (Figure 10). Very little variation is visible along the second PC-axis (9.17%). The postzygapophyses point slightly more outward for higher PC2 scores.

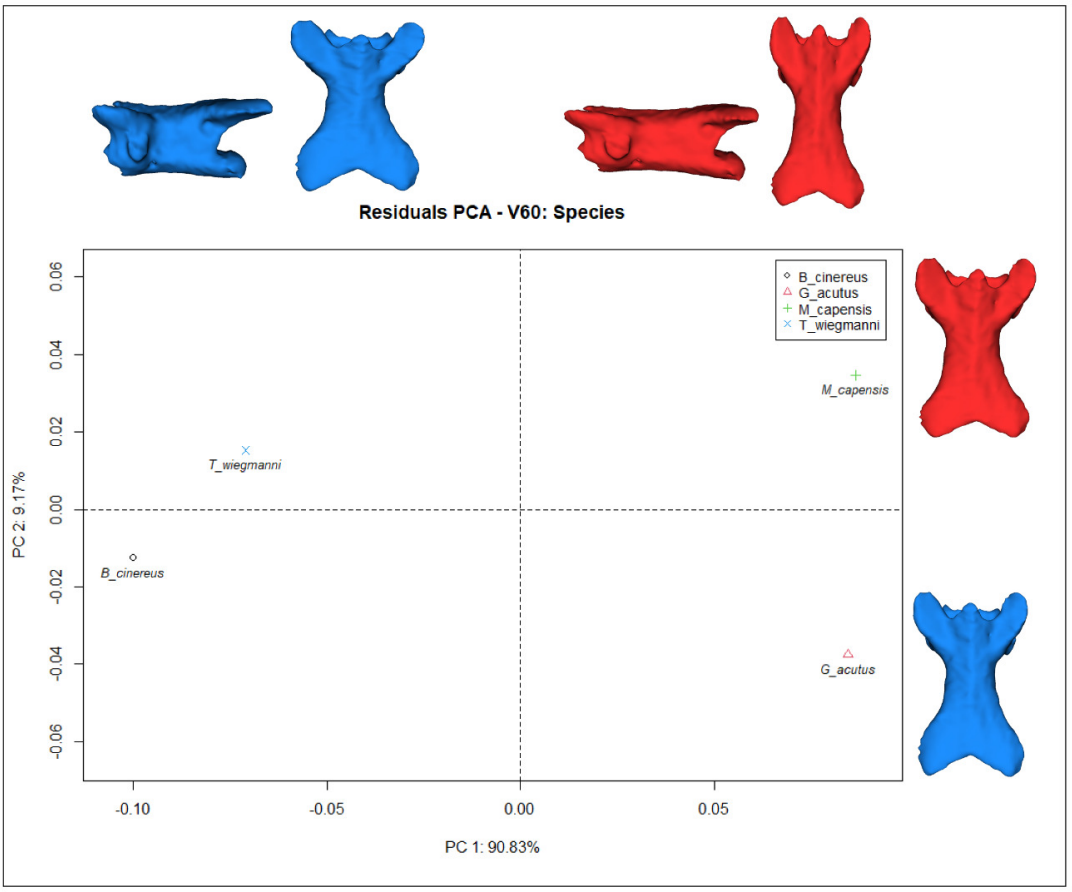

Figure 10: Major axes of V60 shape variation. Blue: warped surfaces representing minimum shapes for the first two PC's. Red: warped surfaces representing maximum shapes.

Morphospace of caudal vertebrae

The first two principal components together account for the total variation found in the caudal vertebrae (summed they explain 100% of the total variation; Figure 11). The first PC shows variation in length, width and orientation of the haemal arch, and length and width of the vertebral main body. A higher value for PC1 suggests a longer and more slender haemal arch, pointing more posteriorly. The vertebral body becomes compressed in length, with prezygapophyses pointing more laterally.
PC2 describes a subtle change in the postzygapophyses: higher PC2 scores show postzygapophyses oriented more posteriorly and being slightly elongated, reaching beyond the neural spine.

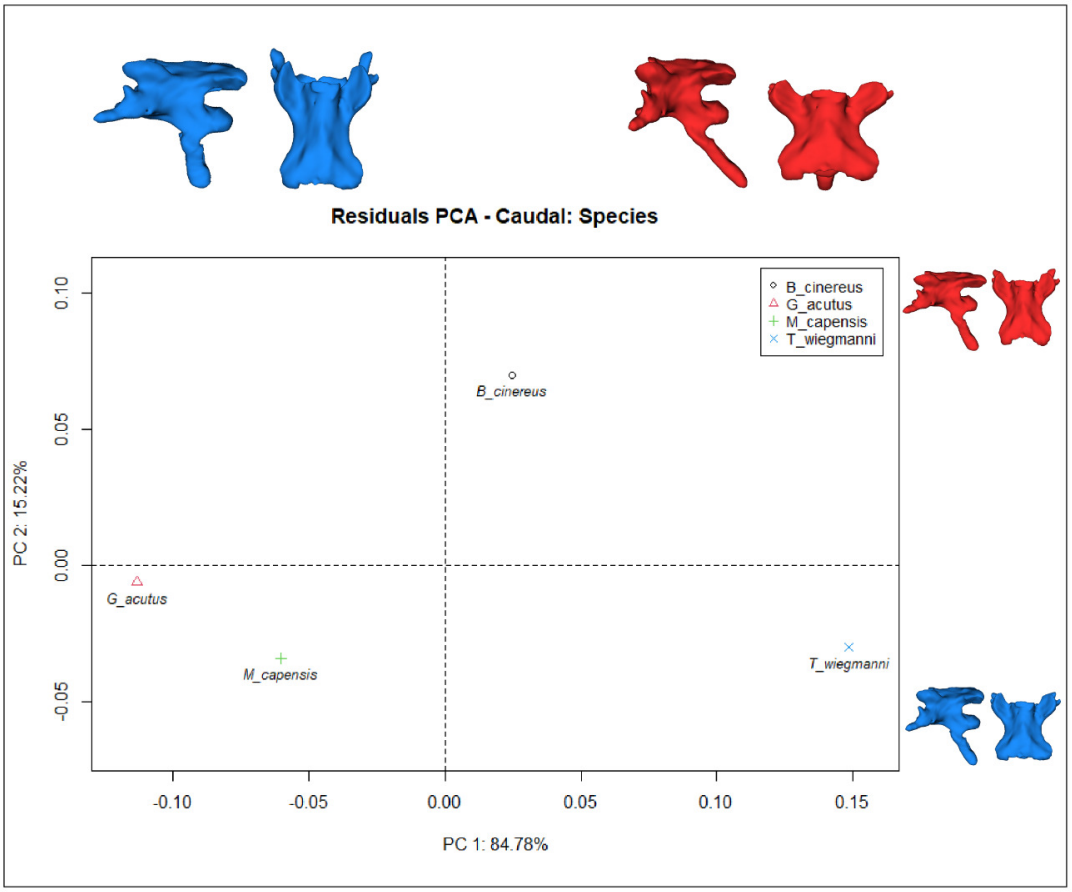

Figure 11: Major axes of caudal shape variation. Blue: warped surfaces representing minimum shapes for the first two PC's. Red: warped surfaces representing maximum shapes.

Morphospace of all post-atlas-axis vertebrae (V3, V20, V60 & Caudal)

This morphospace depicts axes of shape variation for the main vertebral bodies of V3 through caudal vertebrae. Vertebral 'type' specific elements like hypapophyses were excluded. In this morphospace, a nice trend becomes apparent: from low to high PC1 scores, species' vertebral shapes of V3, V20 and V60 are repeatedly ordered as *M. capensis* (shovel), *G. acutus* (keel), *B. cinereus* (round) and *T. wiegmanni* (spade). This PC describes variation in anteroposterior compression (or: elongation for more negative PC1 scores) and the position of the postzygapophyses. The (post)zygapophyseal facets are inclined for most vertebrae, with outer margins lying higher than the base of each facet: if you would expand the facets' surfaces, they would form a 'V'. By contrast, the facets of V3 vertebrae lie horizontal, i.e. parallel to the sagittal plane. Along the vertebral column, accordingly for lower scores of PC1, vertebrae become more elongated. An exception to this trend, and to the interspecies trend, are the caudal vertebrae: these are no longer ordered as *M. capensis, G. acutus, B. cinereus, T. wiegmanni*, nor are they the most elongated, despite their most posterior position in the vertebral column.

PC2 shows variation in the neural spine, which becomes elevated with higher PC2-scores. Likewise, species seem to be similarly ordered as for PC2, with *B. cinereus* and *T. wiegmanni* occuring in the morphospace with lowest scores relative to the other species, for each vertebral type. These low PC2 scores correspond to having a relatively low neural spine, whereas higher scores are found for *M. capensis* and *G. acutus*, tending towards an elevated neural spine.

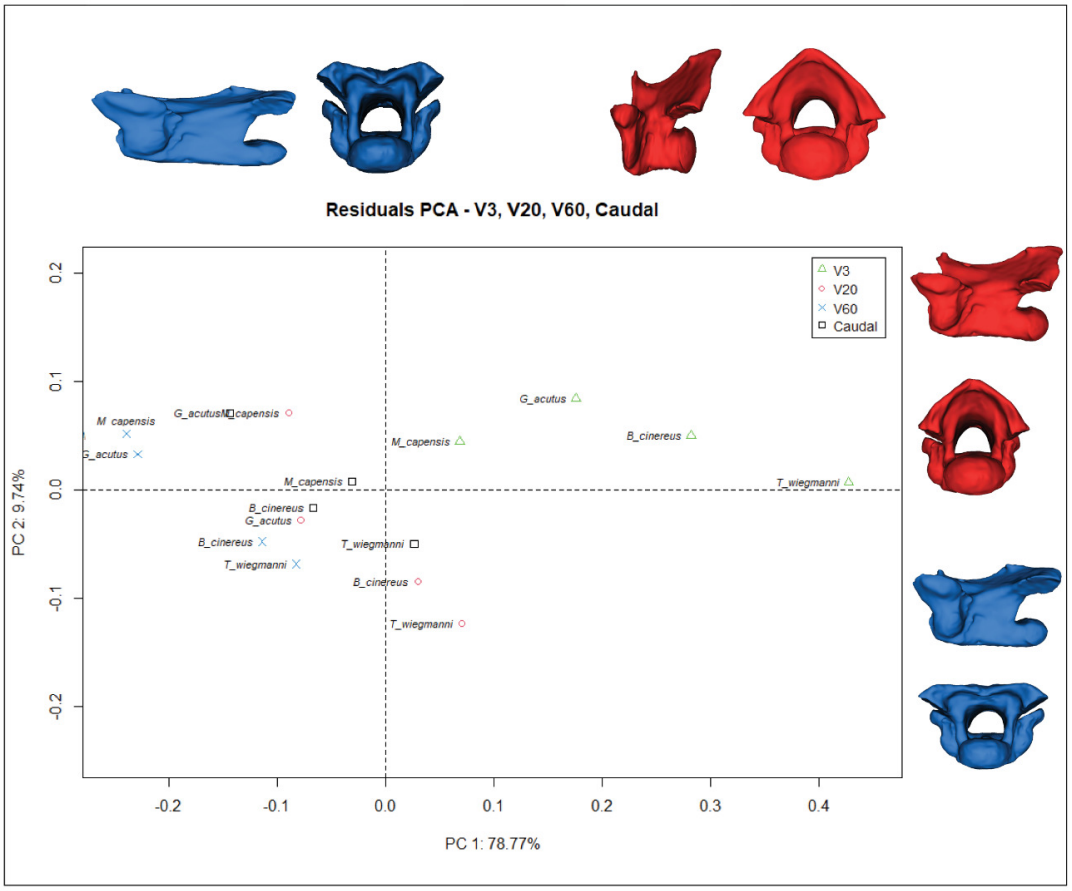

Figure 12: Major axes of shape variation of post-atlas-axis vertebrae. Blue: warped surfaces representing minimum shapes for the first two PC's. Red: warped surfaces representing maximum shapes.

Burrowing trials

The mean burrowing forces for each species are found in Table 1. Our round-headed specimens (*Blanus cinereus*) produced the lowest forces, with an average force of 3.76N. The shovel-heads, *Monopeltis capensis*, achieved an average force of 7.47N, the keel-headed *Geocalamus acutus* of 9.32N. The highest forces were generated by *Trogonophis wiegmanni*: 12.81N. Caution should be taken when interpreting the mean burrowing forces, since only 1 individual was tested in both *M. capensis* and *T. wiegmanni*.

Table 1: Mean burrowing force (N) + standard deviations for each morphotype, represented by its *species*. Between brackets are the number of specimens subjected to the burrowing trials.

Morphotype - *species* (number of specimens)	**Average force (N) ± SD**
Round - *Blanus cinereus* (11)	3.74 ± 1.34
Keel - *Geocalamus acutus* (26)	9.32 ± 2.76
Shovel - *Monopeltis capensis* (1)	7.47 ± 0
Spade - *Trogonophis wiegmanni* (1)	12.81 ± 0

Statistical analysis

We performed linear regression to research the relation between forces and each body measurement. This resulted in both mass and head height (HH) being significantly correlated to burrowing force (R^2 = 0.92 for mass; R^2 = 0.99 for HH; both p-values were 0.0255; Table 2). Mass was measured on dried specimens. Not all specimens were equally shriveled, hence specimens of a similar size could differ in volume. In extreme cases, the vertebral column outlines were visible through the skin. These very dried specimens were not measured, but since a wide range between 'voluminous' and 'shriveled' specimens could confound the measurements of weight, little credibility should be given to the statistical outcomes concerning mass. Therefore, further analysis was done to research correlation between vertebral shapes & burrowing force with head height only. The relation between head height and push force is positive: specimens with higher heads produced higher burrowing forces (Figure 13).

Multivariate linear regression of Procrustes shape coordinates vs. head height and force (with interaction) showed no significant results for all vertebrae (p-values for each vertebral 'type' > 0.05). R^2- and p-values are listed in Table A5.

No significant correlation was found between vertebral shape and burrowing force for any of the vertebrae researched, neither for the raw shapes nor when shapes were adjusted for overall size (Table 3&4; all p-values > 0.05, ranging up to 0.98). Only after adjusting both vertebral shapes and burrowing forces with head height, up to 82% of variation of the push forces is explained by the shapes of the atlas, similarly the axis (R^2 = 0.82 for the atlas, R^2 = 0.81 for the axis; both p-values = 0.026; Table 5). Above 66% of the vertebral shape variation of V3 and V20 is correlated with push forces, however the p-values are borderline non-significant (p = 0.077). Thus, when the atlas resp. axis is scaled for head height, there is a significant correlation between their shape and push force produced by their corresponding specimens. Correlation between HH-adjusted vertebral morphology and push forces becomes insignificant for vertebrae at 60% of the total number of vertebrae and beyond (i.e. the caudal vertebrae) (p-values > 0.15).

Table 2: Results of linear regression between push force and body measurements. Green background filling indicates significant results.

	R^2	F	Z	Pr(>Z)
Mass (g)	0.915	21.628	1.949	0.0255
SVL (mm)	0.102	0.228	-0.440	0.7575
Total length (mm)	0.090	0.198	-0.663	0.7575
Body width (mm)	0.702	4.712	0.860	0.214
Body height (mm)	0.897	17.357	1.528	0.0715
Head length (mm)	0.077	0.166	-0.386	0.6935
Head width (mm)	0.583	2.792	0.612	0.3295
Head height (mm)	0.988	166.75	2.118	0.0255

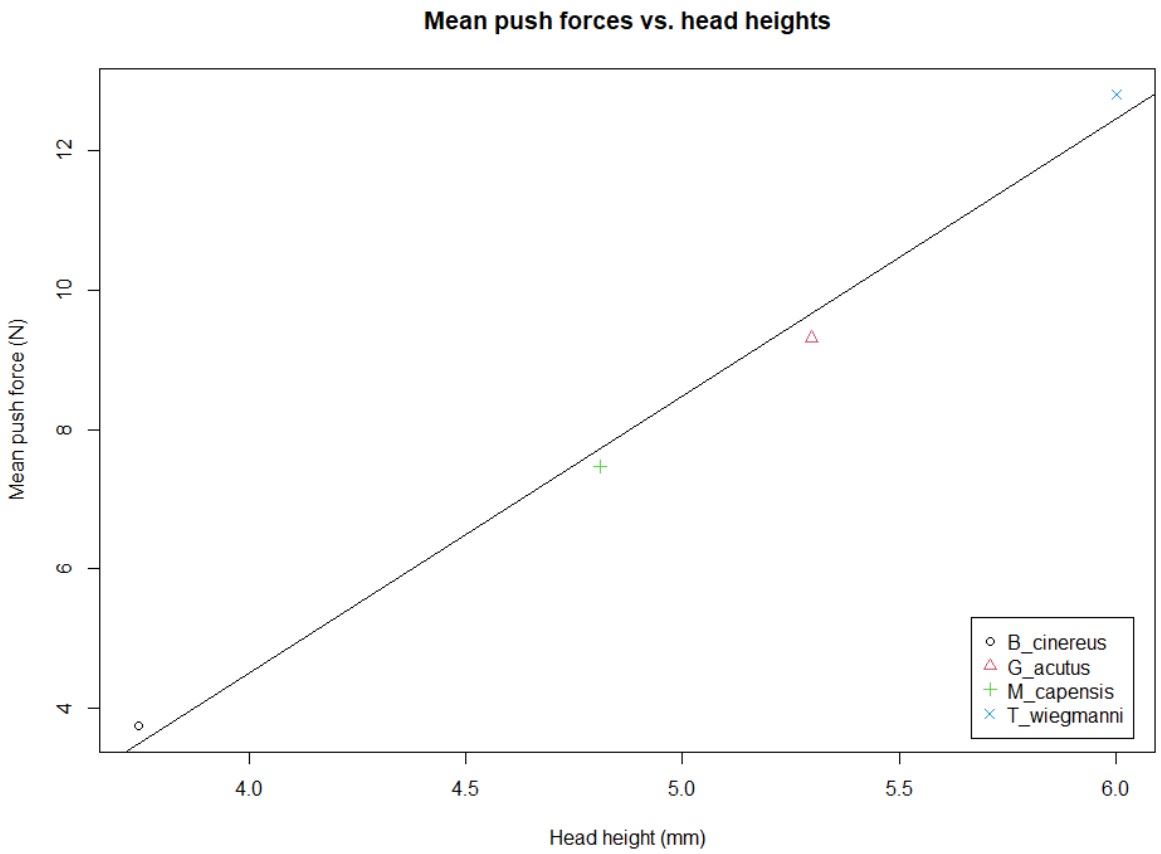

Figure 13: Mean push forces (N) plotted against average head height for all four species.

Table 3: Results for vertebral shapes (not adjusted for overall size) regressed against push force.

	R^2	F	Z	P
V1	0.178	0.432	-0.775	0.7255
V2	0.144	0.336	-0.953	0.8155
V3	0.079	0.170	-1.449	0.9755
V20	0.0748	0.1616	-1.545	0.9755
V60	0.149	0.3498	-1.125	0.8015
Caudal	0.1078	0.242	-1.929	0.9375

Table 4: Results for vertebral shapes (adjusted for overall size) regressed against push force.

	R^2	F	Z	P
V1	0.360	1.127	0.298	0.4345
V2	0.521	2.176	0.854	0.154
V3	0.544	2.382	0.848	0.2675
V20	0.0577	0.122	-1.279	0.8995
V60	0.123	0.280	-0.835	0.837
Caudal	0.155	0.366	-0.554	0.7905

Table 5: Linear regression of the residuals of the vertebral Procrustes shape coordinates vs. force, i.e. adjusted for head height. Green background filling indicates significant results.

	R^2	F	Z	P
V1	0.815	8.810	1.776	0.0255
V2	0.811	8.583	1.791	0.0255
V3	0.684	4.322	1.669	0.0765
V20	0.665	3.966	1.598	0.0765
V60	0.469	1.768	1.007	0.1675
Caudal	0.424	1.470	0.614	0.2644

Discussion

Comparison of cervical vertebrae in (V1, V2, V3)

Although not visible from the atlas PCA, the spade-headed *T. wiegmanni* is the sole species whose atlas has prominent (though vestigial) transverse processes. *T. wiegmanni* relies on head rotation relative to the body for scraping off soil from the tunnel walls while burrowing (C. Gans, 1974). The moment arm would become too short to produce such movements if transverse processes were absent (Čerňanský & Stanley, 2019). Lateral processes in our shovel-head, which relies on vertical head movements while burrowing, are as good as absent.

Vestigial structures for prezygapophyses of the axis are found in the round-head *B. cinereus* and, less prominent, in the keel-headed *G. acutus*. In lepidosaurs these prezygapophyses articulate with postzygapophyses of the atlas, locking them and impeding head inclination and lateral rotation. The articulation becomes lost upon transition to a serpentiform morphology (A. Čerňanský, 2016). The two species that completely lack such zygapophyses, the shovel- and spade-headed *M. capensis* and *T. wiegmanni* resp., both rely on movements that the articulation would otherwise make impossible (i.e. upward and oscillatory movement resp.).

As expected, the third intercentrum (or hypapophysis) of the axis of our shovel-head (*M. capensis*), is very short and is therefore unlikely to interfere with their ventrad head-movement when burrowing. A similar trend is found for the hypapophysis of the third vertebra. The burrowing methods in round- (*B. cinereus*) and keel-headed types (*G. acutus*), being forward pushing and lateral movement resp., are not hindered by their long, horizontal hypapophysis. The hypapophysis of our spade-snout (*T. wiegmanni*) is inclined ventrally, leaving more space for oscillatory movement of the neck without blocking it.

Comparison of post-atlas-axis vertebrae (V3, V20, V60, Caudal)

Along the main axes of variation in the morphospace of V3 through caudal vertebrae (Figure 17), three characteristics show principal variation: length of vertebrae and position of the zygapophyseal facets and height of the neural spine.

‘V’-shaped zygapophyseal facets are found for most of the vertebrae except for V3 (Figure 12). Horizontal zygapophyseal would permit for increased torsional capacity, i.e. the rotation along the craniocaudal axis of each vertebra relative to each other. As all V3 vertebrae are found in the morphospace at the site indicating such horizontal facets, torsional movements are likely possible in the cervical area of all morphotypes. The degree to which torsion could occur might be different for each morphotype. According to its position in the morphospace, the highest degree of torsion is likely possessed by the spade-headed *T. wiegmanni.* Having oscillatory burrowing locomotion is enabled by

it's horizontal facets. However, as Kuznetsov & Tereschenko (2010) state, deriving a degree of torsion solely based on skeletal tissue, without integration of surrounding soft tissue, is impossible.

For PC1, for each vertebra 'type', the spade-snout (*T. wiegmanni*) is repeatedly found at the maximal end of the axis, represented by a compressed vertebral body and horizontal zygapophyseal facets. Body elongation is described by C. Gans (1974) as having an "elongated trunk and number of vertebrae ranging between 100 and 300 or more". *T. wiegmanni*, our specimen has only 84 vertebrae (Table A4), is consequently considered showing reversal of bodily elongation (C. Gans, 1974).

V3 and V20 of different morphotypes show variation in their neural spine, whereas the neural 'spines', or better, the neural ridges, differ little in V60 and caudal vertebrae according to their morphospaces (Figures 8-11). V20, V60 and caudal vertebrae cluster somewhat together in the post-atlas-axis morphospace, having almost flattened neural arches (Figure 12), whereas V3 vertebrae show a more distinctive elevation of the neural ridge anterior tip.

The caudal vertebrae additionally shows variation in the length and orientation of the haemal arch (Figure 11). To elucidate the morphofunctional traits of these caudal morphotypes and whether it has a role in burrowing tactics, it is suggested to research its muscular associations. In limbed, *m. caudofemoralis longus* is attached to the sides of the haemal arch. As described by Westphal *et al.* (2019), limb-associated muscles are known to have changed insertion sites and, ofcourse, function. The role of this and other caudal muscles might be interesting in the spade-head (*T. wiegmanni*), which is the sole amphisbaenian that uses his tail for at least part of the burrowing process.

Conclusion

Of our four morphotypes, the considered least-specialized morphotype (round) produced the lowest burrowing forces. Unexpectedly, *M. capensis* (shovel), considered the most specialized for burrowing, produced second lowest burrowing forces. Our spade-headed specimens (*T. wiegmanni*), produced the highest forces.

Main variation of the atlas occurs in its height-to-width ratio. Head height was found to be positively correlated with burrowing forces. Morphotypes with the highest height-to-width ratio, i.e. the most dorsoventrally stretched atlases were found to produce the highest burrowing forces (keel & spade morphotypes, represented by *G. acutus* and *T. wiegmanni* respectively).

Our spade-headed species, *T. wiegmanni,* likely has a relatively highly flexible neck, as suggested by several characteristics found in its skeletal bridge. For instance, the zygapophyseal facets of the axis lie parallel to the sagittal plane, which implies possible torsional movements of vertebrae relative to each other. Similarly, the intercentrum of the axis leaves sufficient space for downward extension of the head. Shovel-heads, which rely on up- and downward movement of the head, have an axis intercentrum that does not restrict the downward head tilt. A dorsoventrally compressed condyle is indicative of movement perpendicular to its long axis. Although variation of condyle shape found little support in our morphospaces, concerning main cranial movements, expected condyle shapes are found for all four species (particularly for shovel-, spade- and round-snouts; Figure A3).

In this study, morphofunctional implications were made solely based on osteological tissues. Since associated muscles are crucial in burrowing locomotion, it would be advised to research both muscular and skeletal variation between different morphotypes and their interactive role in burrowing.
The presence of internal concertina locomotion has only been tested for one amphisbaenian species. Since amphisbaenians show several characteristics that would allow for internal concertina, and this locomotion could possibly play an important role in the burrowing performances of different

morphotypes, researching internal concertina locomotion in amphisbaenians seems indispensable to unravel the many questions surrounding their morphofunctional adaptations to burrowing.

Summary English

Amphisbaenians are limbless, fossorial reptiles. They have peculiar, distinct cranial shapes or morphotypes, each corresponding to a specialized mode of burrowing. Similarly, species' postcranium is expected to be adapted to its applied mode of burrowing, as with a head along you won't dig deep. Elongation and addition of the vertebrae are usually found in limbless fossorial species, but descriptions of further vertebral adaptations are so far limited.
We used landmark based 3D geometric morphometric analysis to determine the main axes of variation in vertebral shapes. Hereto, four amphisbaenians - *Blanus cinereus, Trogonophis wiegmanni, Geocalamus acutus* and *Monopeltis capensis* - representing four different cranial morphologies, each with its own burrowing method, were subjected to burrowing trials to detect push forces (following a method described by Vanhooydonck *et al., 2011*). Morphometric data on the body were collected. Of each of the four morphotypes, μCT-scans of six vertebrae (the atlas, axis, third cervical vertebrae, vertebrae at 20% and 60% of the total number of vertebrae, and caudal vertebrae) were segmented and landmarked (using Stratovan). Linear regression analyses were used to evaluate the covariation between body measurements, vertebral shapes and burrowing forces.

The spade-headed morphotype produced the largest burrowing forces (12.8N), followed by the keel- (9.3N), shovel (7.5N) and last round-headed morphotype (3.7N).

The atlases of each morphotype varied mainly in their height-to-width ratio, whereas post-atlas vertebrae varied in length-to-width ratio. *T. wiegmanni* was found to have the shortest vertebrae. An interesting principal component of variation occurs in the zygapophyseal facets: horizontally oriented, they allow for torsional movement of one vertebrae to another. Such facets were found for the morphotype heavily relying on such torsional movement while burrowing (the spade-snouted type). The intercentrum of the axis seems to show morphology adaptive to its associated burrowing method: short or ventrally oriented intercentra permit greater flexibility between vertebrae and were found for the shovel and spade morphotypes, which both require sufficient downward inclination of the head while burrowing.

Future research implementing musculature and the possible use of internal concertina locomotion could further elucidate the still many remaining questions concerning amphisbaenians peculiar burrowing locomotion.

Summary Dutch

Amphisbaenia zijn pootloze, gravende reptielen. Ze bezitten eigenaardige kop-morfologieën of 'morphotypes', elk gespecialiseerd naar een bijhorende aparte graafmethode. Evenredig wordt verwacht dat het postcranium aan de typische graafmethode is aangepast. Elongatie en additie van ruggenwervel is een typisch wederkerend patroon in pootloze, gravende soorten; verder is er een gebrekkige hoeveelheid informatie over adaptaties in de ruggenwervelkolom.
Bij deze trachten wij met deze studie een vergelijkende beschrijving te geven over de mogelijke postcraniale adaptaties voor graafmethodes in Amphisbaenia.
3D Geometric Morphometric analyse werd toegepast zodanig de meest prominente variaties in ruggenwervel-vormen te beschrijven. Hiertoe werden vier Amphisbaenia species, representatief voor de vier hoofdzakelijke morfotypes, onderzocht (*B. cinereus* (ronde kopvorm)*, G. acutus* (kielvormig)*, M. capensis* (schopvormig)*, T. wiegmanni* (spade-vormig)). Zij werden onderworpen aan graaf-proeven, zodanig hun respectievelijke graafkrachten (in Newton) uiteen te zetten (volgens de

methode beschreven door Vanhooydonck *et al.,* 2011). Morfometrische data omtrent hun lichaam werden verzameld. Van een individu van elk morfotype werden μCT-scans genomen van zes ruggenwervels (de atlas, axis, derde nekwervel, ruggenwervels gelegen op 20% en 60% van de totale aantal wervels, en een staartwervel). De scans werden gesegmenteerd en gelandmarked (via Stratovan) voor vergelijkende vorm-onderzoek (PCA, Principle Component Analysis). Lineaire regressie analyse werd toegepast om de relaties tussen de wervel-vormen, de lichaamsafmetingen en de graafkrachten in kaart te brengen.

De spade-morfotype produceerde the hoogste graafkracht (12.8N), gevolgd door de kiel- 9.3N), shovel- (7.5N) and als laatste de rondkoppige morfotype (3.7N).

Verder onderzoek op de aanwezigheid van interne concertina, includerend spier-morfologie en -functies, kan helpen resterende vragen uit te klaren.

Acknowledgment

I'd like to thank my supervisor, prof. dr. Dominique Adriaens and my counsellor, Aurélien Lowie, for their many and late-hour help. I'd like to thank Aurélien especially for guiding me every step along the way. Every (online) meeting has put my mind a bit more at ease. I should also thank Julie Moana Mede Moussa, a fellow student, for her help, friendly support and the many on- and off-topic smiles. Further, I'd like to thank Anthony Herrel for providing the specimens. I'm grateful for having had the opportunity to work on this thesis.

References

1. Boszczyk, B. M., Boszczyk, A. A., & Putz, R. (2001). Comparative and functional anatomy of the mammalian lumbar spine. *The Anatomical Record: An Official Publication of the American Association of Anatomists*, *264*(2), 157-168.
2. Čerňanský, A. (2016). From lizard body form to serpentiform morphology: The atlas–axis complex in A frican cordyliformes and their relatives. *Journal of morphology*, *277*(4), 512-536.
3. Čerňanský, A., & Stanley, E. L. (2019). The atlas–axis complex in Dibamidae (Reptilia: Squamata) and their potential relatives: The effect of a fossorial lifestyle on the morphology of this skeletal bridge. *Journal of morphology*, *280*(12), 1777-1797.
4. Čerňanský, A., Yaryhin, O., Ciceková, J., Werneburg, I., Hain, M., & Klembara, J. (2019). Vertebral comparative anatomy and morphological differences in anguine lizards with a special reference to Pseudopus apodus. *The Anatomical Record*, *302*(2), 232-257.
5. Gans, C. (1978). The characteristics and affinities of the Amphisbaenia. *The Transactions of the Zoological Society of London*, *34*(4), 347-416.
6. Gans, C. (1974). Biomechanics: Approach to vertebrate Biology. J. P. Lippincott, Philadelphia.
7. Herrel, A., & Measey, G. J. (2010). The kinematics of locomotion in caecilians: effects of substrate and body shape. *Journal of Experimental Zoology Part A: Ecological Genetics and Physiology*, *313*(5), 301-309.
8. Hipsley, C. A., Rentinck, M. N., Rödel, M. O., & Müller, J. (2016). Ontogenetic allometry constrains cranial shape of the head‐first burrowing worm lizard Cynisca leucura (Squamata: Amphisbaenidae). *Journal of morphology*, *277*(9), 1159-1167.
9. Hohl, L. D. S. L., de Castro Loguercio, M. F., Sicuro, F. L., de Barros-Filho, J. D., & Rocha-Barbosa, O. (2017). Body and skull morphometric variations between two shovel-headed species of Amphisbaenia (Reptilia: Squamata) with morphofunctional inferences on burrowing. *PeerJ*, *5*, e3581.
10. Hohl, L. S. L., Loguercio, M. F. C., Buendía, R. A., Almeida‐Santos, M., Viana, L. A., Barros‐Filho, J. D., & Rocha‐Barbosa, O. (2014). Fossorial gait patterns and performance of a shovel‐headed amphisbaenian. *Journal of Zoology*, *294*(4), 234-240.

11. Kearney, M., & Stuart, B. L. (2004). Repeated evolution of limblessness and digging heads in worm lizards revealed by DNA from old bones. *Proceedings of the Royal Society of London. Series B: Biological Sciences*, *271*(1549), 1677-1683.
12. Kuznetsov, A. N., & Tereschenko, V. S. (2010). A method for estimation of lateral and vertical mobility of platycoelous vertebrae of tetrapods. *Paleontological Journal*, *44*(2), 209-225.
13. Moon, B. R. (1999). Testing an inference of function from structure: snake vertebrae do the twist. *Journal of Morphology*, *241*(3), 217-225.
14. Navas, C. A., Antoniazzi, M. M., Carvalho, J. E., Chaui-Berlink, J. G., James, R. S., Jared, C., Kohlsdorf, T., Dal Pai-Silva M. & Wilson, R. S. (2004). Morphological and physiological specialization for digging in amphisbaenians, an ancient lineage of fossorial vertebrates. *Journal of Experimental Biology*, *207*(14), 2433-2441.
15. Otero, A., Gallina, P. A., Canale, J. I., & Haluza, A. (2012). Sauropod haemal arches: morphotypes, new classification and phylogenetic aspects. *Historical Biology*, *24*(3), 243-256.
16. Summers, A. P., & O'Reilly J. C. (1997). A comparative study of locomotion in the caecilians Dermophis mexicanus and Typhlonectes natans (Amphibia: Gymnophiona). *Zoological Journal of the Linnean Society*, *121*(1), 65-76.
17. Vander Linden, A., Campbell, K. M., Bryar, E. K., & Santana, S. E. (2019). Head‐turning morphologies: Evolution of shape diversity in the mammalian atlas–axis complex. *Evolution*, *73*(10), 2060-2071.
18. Vanhooydonck, B., Boistel, R., Fernandez, V., & Herrel, A. (2011). Push and bite: trade-offs between burrowing and biting in a burrowing skink (Acontias percivali). *Biological Journal of the Linnean Society*, *102*(1), 91-99.
19. Westphal, N., Mahlow, K., Head, J. J., & Müller, J. (2019). Pectoral myology of limb-reduced worm lizards (Squamata, Amphisbaenia) suggests decoupling of the musculoskeletal system during the evolution of body elongation. *BMC evolutionary biology*, *19*(1), 1-23.